Z. Physik 257, 147–176 (1972)

Experimental Study of High Spin States in the Ground State Bands of $^{158,160}Er$, $^{164,166}Yb$, and ^{168}Hf

R. M. Lieder, H. Beuscher, W. F. Davidson, P. Jahn, H.-J. Probst, and C. Mayer-Böricke

Institut für Kernphysik der Kernforschungsanlage Jülich

Received September 21, 1972

Ground state rotational bands in the deformed doubly-even rare earth nuclei $^{158,160}Er$, $^{164,166}Yb$, and ^{168}Hf have been observed in (α, $8n\gamma$) reactions. The γ-spectra associated with these reactions were studied in-beam using conventional spectroscopic methods. In all five nuclei the nuclear moment of inertia of the ground state rotational states was found to increase abruptly as higher spin states were attained. In a plot of the moment of inertia as a function of the angular velocity all these five nuclei display "backbending" curves. Moreover, in ^{158}Er and ^{166}Yb, the curves after passing through a maximum bend subsequently downwards.

1. Introduction

The study of the ground state bands (hereafter denoted gsb) in deformed doubly-even rare earth nuclei has in recent times received renewed interest following the discovery by a Swedish group[1] that in the nuclei $^{158,160}Dy$ and ^{162}Er the nuclear moment of inertia increases drastically as higher spin states are reached. This fact can be experimentally observed from the γ-ray spectrum where the transitions up to the 10^+ state or thereabouts are spaced at approximately equidistant intervals but beyond this the transition energies tend to converge, as in ^{160}Dy, or even to decrease, as in ^{162}Er.

This behaviour of the moment of inertia was first predicted theoretically in 1960 by Mottelson and Valatin[2]. In deformed nuclei the moment of inertia associated with the ground state is about one third of the value for rigid rotors. This is attributed to the existence of pairing correlations. However as higher angular momenta are reached, the Coriolis forces arising from the nuclear rotation increasingly oppose these pairing forces so that, initially for the neutrons but also later for the protons, the

1 Johnson, A., Ryde, H., Hjorth, S. A.: Nucl. Phys. A **179**, 753 (1972). — Johnson, A., Ryde, H., Sztarkier, J.: Phys. Letters **34** B, 605 (1971).

2 Mottelson, B. R., Valatin, J. G.: Phys. Rev. Letters **5**, 511 (1960).

pairing correlations are reduced and vanish at a particular critical angular momentum, which was originally estimated[2] to be 12 $\hbar$ for $A \approx 180$. As a result of this Coriolis anti-pairing effect (the CAP effect), the moment of inertia tends towards the rigid rotor value. More recent calculations[3-5] indicate that the critical angular momentum for neutrons lies in the range $12 \rightarrow 24\ \hbar$.

The manner in which the moment of inertia θ tends towards the rigid rotor value as higher spin values are reached can be very different from nucleus to nucleus, and has so far been represented in a plot θ vs. ω^2, where ω has been defined as the angular velocity of the nucleus[1]. In such plots ^{162}Er displays a "back-bending" characteristic. Possible theoretical descriptions of the back-bending effect have been proposed on the basis of the CAP effect by Krumlinde and Szymanski[6], and also by Sorensen[7], and Kumar[8].

A different approach to the problem of the back-bending effect has been adopted by Stephens and Simon[9]. In this model the Coriolis effects were investigated at high angular momenta in a system consisting of two (or four) particles in the $i_{13/2}$ shell model state which are coupled to a deformed core. As the angular momentum is increased the particles tend to decouple from the core and their angular momenta are aligned to the total angular momentum of the core.

To test the validity of the above theoretical descriptions, experiments were initiated in this laboratory to study the behaviour of some doubly-even rare earth nuclei at high spin states. Similar studies have been carried out by Thieberger *et al.*[10] on ^{158}Dy, where states up to 22^+ have been identified, by Mo *et al.*[11] on ^{168,170,172}Yb, and by Taras *et al.*[12] on the transitional nucleus ^{132}Ce.

Recently it has been noted that in some doubly-even nuclei in the $2s-1d$ shell an anomaly similar to the back-bending behaviour

3 Faessler, A., Greiner, W., Sheline, R. K.: Nucl. Phys. **62**, 241 (1965).
4 Krumlinde, J.: Nucl. Phys. A**160**, 471 (1971).
5 Sano, M., Wakai, M.: Progr. Theoret. Phys. (Kyoto) **47**, 880 (1972).
6 Krumlinde, J., Szymanski, Z.: Phys. Letters **36** B, 157 (1971).
7 Sorensen, R. A.: Proc. of the Colloquium on intermediate nuclei, Orsay, p. 70, July 1971.
8 Kumar, K.: Contribution to the Symposium on High Spin Nuclear States and Related Phenomena, Stockholm 1972.
9 Stephens, F. S., Simon, R. S.: Nucl. Phys. A**183**, 257 (1972).
10 Thieberger, P., Sunyar, A. W., Rogers, P. C., Lark, N., Kistner, O. C., der Mateosian, E., Cochavi, S., Auerbach, E. H.: Phys. Rev. Letters **28**, 972 (1972).
11 Mo, J. N., Chapman, R., Dracoulis, G. D., Gelletly, W., Hartley, A. J.: Communication to the European Conference on Nuclear Physics, Aix-en-Provence, p. 101, 1972.
12 Taras, P., Dehnhardt, W., Mills, S. J., Veggian, M., Merdinger, J. C., Neumann, U., Povh, B.: Phys. Letters **41 B**, 295 (1972).

exists[13,14]. In these nuclei the many body problem has been solved realistically using angular momentum projection before Hartree-Fock-Bogoliubov variation. These calculations give reasonably quantitative agreement with the experimental data[13].

Short communications on the back-bending behaviour observed in ^{164}Yb and ^{168}Hf, and in ^{158}Er and ^{166}Yb have been published from this laboratory in the literature[15,16]. A brief report on the present work was presented at the Symposium on High Spin Nuclear States and Related Phenomena in Stockholm[17].

2. Experimental Methods

In the measurements reported here self-supporting metallic foils were used, which were prepared from enriched rare earth isotopes in oxide form obtained from Oak Ridge National Laboratory. These isotopes and their respective enrichments are given in Table 1. The rare earth oxides were reduced in vacuo with either lanthanum or thorium metal at high temperature[18] produced by focussing an electron beam onto a tantalum crucible. The reduced material was evaporated onto thin tantalum sheeting which was subsequently dissolved in an equal mixture of fluoric and nitric acids. The resulting target foil was mounted onto an aluminium frame. The thickness and surface area of these foils were $\approx 4\ \mathrm{mg/cm^2}$ and $8\ \mathrm{mm} \times 12\ \mathrm{mm}$ respectively.

The targets were bombarded with the external α-beam from the Jülich isochronous cyclotron JULIC. To produce the final nuclei under investigation α-energies between 100 and 112 MeV were used so that the

Table 1

Target	^{162}Dy	^{164}Dy	^{168}Er	^{170}Er	^{172}Yb
Enrichment	96.3%	98.4%	99.9%	96.9%	91.5%

13 Goeke, K., Müther, H., Faessler, A.: Nucl. Phys. (to be published). — Faessler, A., Goeke, K., Müther, H.: Contribution to the Symposium on High Spin Nuclear States and Related Phenomena, Stockholm 1972.

14 Sheline, R. K.: Contribution to the Symposium on High Spin Nuclear States and Related Phenomena, Stockholm 1972.

15 Lieder, R. M., Beuscher, H., Davidson, W. F., Jahn, P., Probst, H.-J., Mayer-Böricke, C.: Phys. Letters **39** B, 196 (1972).

16 Beuscher, H., Davidson, W. F., Lieder, R. M., Mayer-Böricke, C.: Phys. Letters **40** B, 449 (1972).

17 Lieder, R. M., Beuscher, H., Davidson, W. F., Jahn, P., Probst, H.-J., Mayer-Böricke, C.: Contribution to the Symposium on High Spin Nuclear States and Related Phenomena, Stockholm 1972.

18 Westgaard, L., Bjornholm, S.: Nucl. Instr. **42**, 77 (1966).

(α, 8n) reaction predominated. The beam spot at the target was 2 mm in diameter and the beam currents ranged from 10 pA for coincidence measurements to 3 nA for γ-singles experiments.

The γ-radiation from the final nucleus was studied using conventional in-beam spectroscopic methods. The collected data consisted of γ-singles spectra, γ-spectra time related to the beam bursts of the cyclotron, γ-ray angular distributions and $\gamma\gamma$-coincidence spectra.

In the measurement of γ-singles spectra, and of γ-ray angular distributions with respect to the beam direction, a cylindrical aluminium target chamber with a thin wall was used. This chamber was mounted centrally on an angular distribution table. A Ge(Li) detector 20 cm distant from the target could be rotated about the target position from 90° to 150° in 15° steps. Since the Ge(Li) detector was shielded with a lead cone more backward angles could not be reached. Either a one open end coaxial Ge(Li) detector of 66 cm^3 sensitive volume (11.7% relative efficiency) or a planar 0.7 cm^3 Ge(Li) detector with resolutions respectively of 2.4 and 1.4 keV at 661 keV were used. A second Ge(Li) detector was placed at a fixed angle. This monitor detector was used to normalise the γ-spectra measured with the moveable detector at different angles. The output pulses of this detector were used to trigger a pulser whose output was fed into the preamplifier of the moveable detector. In this way a pulser line was produced in the γ-spectrum of the moveable detector which could be used for the normalisation. With this method not only a correction for fluctuating beam current is obtained, but also a correction for dead time losses of the whole electronic system including the multichannel analyser results. The beam was dumped in a well-shielded Faraday cup 3 m downstream from the target.

Measurements of γ-spectra were also carried out in time relationship with the cyclotron beam bursts. These were about 3 ns wide, and had a duty cycle of 45 ns at $E_\alpha = 100$ MeV. To pick up a timing signal from the beam pulses a 0.1 mm scintillator foil viewed by a photomultiplier could be brought into the beam 40 cm behind the target[19]. The γ-radiation emitted from the target was measured in delayed coincidence with the beam bursts. The overall time resolution was 6 ns FWHM for $E_\gamma > 200$ keV. The two-parameter spectra, the parameters being respectively the γ-ray energy and the time elapsed after the beam burst, were recorded event by event on magnetic tape. For these measurements a planar 6 cm^3 Ge(Li) spectrometer with a resolution of 1.6 keV at 661 keV was employed.

The $\gamma\gamma$-coincidence measurements were carried out using two Ge(Li) detectors of 40 cm^3 (6% relative efficiency — true coaxial) and 66 cm^3

19 Warner, R. A., Smith, G. L., Lieder, R. M., Draper, J. E.: Nucl. Instr. **75**, 149 (1969).

(11.7% relative efficiency – one open end coaxial). A small rectangular target chamber was constructed in such a manner that the two Ge(Li) detectors could subtend the maximum achievable solid angles of 11 and 16% respectively. In this way the Ge(Li) counters were positioned opposite each other perpendicular to the beam axis at a distance of 11 mm from the target spot.

During the course of these experiments lead cones were inserted between the detectors thereby decreasing the solid angle but improving the quality of the coincidence spectra very markedly. With this improvement the background in the coincidence spectra was reduced by a factor of two. This background is mainly composed of unresolved γ-rays originating from the feeding into the gsb, and of γ-rays associated with events induced by neutrons evaporated from the compound nucleus. The latter contribution was reduced considerably by introducing the lead cones.

Timing was carried out using ORTEC constant fraction timing discriminator units, giving a resolving time of $2\tau \approx 15$ ns FWHM for all γ-energies above 200 keV. For smaller energies the time resolution deteriorated very rapidly since the 66 cm^3 detector had one open end coaxial geometry. Therefore on setting a window on the prompt peak in the time spectrum, the coincidence efficiency in the interval ranging approximately from 600 to 200 keV reduces gradually with decreasing energy in comparison with the detection efficiency in γ-singles experiments. Below 200 keV the coincidence efficiency falls off rapidly. The coincidence data were stored event by event in 2048×2048 mode on magnetic tape.

The data collected from these experiments were analysed off-line using a PDP-15 computer. To create coincidence spectra associated with one Ge(Li) detector, the two-parameter data were sorted, using a computer code developed in this laboratory, by setting gates on interesting parts of the spectrum associated with the other Ge(Li) detector. Gates were set on all γ-peaks of interest as well as on appropriate portions of background so that background-subtracted coincidence spectra could be obtained. Similar procedures were employed with the two-parameter timing data to obtain either a sequence of prompt and delayed γ-spectra or time spectra of relevant γ-peaks.

All the γ-spectra were analysed using a modified version of the computer code described in Ref. [20]. To determine the areas and locations of the peaks, standard line shapes were fitted to them after subtraction of the background. The standard line shape was composed of a Gaussian curve joined to an exponential tail on the low-energy side of the peak. The shape parameters, viz. Gaussian width and location of the joining

20 Routti, J. T., Prussin, S. G.: Nucl. Instr. **72**, 125 (1969).

point, were determined by analyzing an ^{152}Eu spectrum taken in the experimental geometry.

All γ-ray energies were determined from in-beam spectra taken simultaneously with a ^{152}Eu source whose energies are accurately known[21]. The detection efficiencies for both γ-singles as well as for $\gamma\gamma$-coincidences were obtained from spectra taken with a ^{152}Eu source mounted at the target position. The relative γ-intensities were taken again from Ref.[21].

3. Experimental Results

In this section all experimental data are presented and the procedures used to identify and assign γ-transitions as members of the ground state bands in the nuclei ^{158,160}Er, ^{164,166}Yb, and ^{168}Hf are given.

Before a particular transition can be identified as a transition within the gsb of a given deformed nucleus, certain criteria have to be satisfied. In particular the states of the gsb are connected by stretched $E2$ transitions, and have short lifetimes ranging from a few ns for the 2^+ state down to the ps region for higher spin states[22].

The intensities of the γ-transitions of the gsb are determined by the feeding mechanism which can be described as follows. Bombardment of a target nucleus with 100 MeV alphas leads to the formation of a compound nucleus which decays by evaporation of neutrons and subsequently by γ-decay until the gsb is reached[23]. It was found that γ-ray feeding into the gsb is distributed over a number of levels. Because of this "side-feeding" the intensity of the gsb transitions increases monotonically on cascading down the band. This feature can be used to determine the sequential placement of the gsb transitions, not only from singles spectra but much more effectively from the coincidence spectra.

In the coincidence data a transition is considered as a possible member of the gsb only if it appears in coincidence with all other transitions within the gsb. The sequencing of these transitions is derived from the fact that transitions occurring above a particular gating transition fall off in intensity in the same way as in the singles spectrum, whereas all transitions following the gating transition have uniform intensity since the side-feeding γ-rays to the lower levels are not coincident and thereby do not contribute.

---

21 Riedinger, L. L., Johnson, N. R., Hamilton, J. H.: Phys. Rev. C **2**, 2358 (1970).
22 Diamond, R. M., Stephens, F. S., Kelly, W. H., Ward, D.: Phys. Rev. Letters **22**, 546 (1969).
23 Newton, J. O., Stephens, F. S., Diamond, R. M., Kelly, W. H., Ward, D.: Nucl. Phys. A **141**, 631 (1970).

To verify that a coincident γ-transition belongs to the gsb, the fact that gsb transitions have stretched $E2$ character has to be substantiated. Stretched $E2$ transitions following (α, xn) reactions have angular distributions with strong positive anisotropies. This takes place because the compound nucleus is completely aligned by the reaction in the plane perpendicular to the incoming beam and this alignment is preserved to a large extent during the deexcitation into the gsb. In addition it has been found that due to the side-feeding these anisotropies diminish gradually as the transitions cascade down the gsb[24]. This effect is again of assistance in verifying the sequential ordering of the gsb transitions.

To exclude the possibility that a given γ-transition considered to belong to the gsb cascade deexcites an isomeric state, it has to be shown that this transition appears promptly with respect to the beam bursts.

Finally it should be emphasised that the ultimate assignment of transitions to the gsb of the five nuclei considered in the present work was only accomplished after a careful appraisal of all the above-mentioned procedures and arguments.

3.1. The Nucleus ^{158}Er

Information concerning the gsb in ^{158}Er up to the 12^+ state has been reported previously from Berkeley[22,25,26].

A typical γ-singles spectrum of the ^{162}Dy$(\alpha, xn\gamma)$ reaction at $E_\alpha =$ 100 MeV taken with the 6 cm^3 Ge(Li) detector is displayed in Fig. 1. The yield for the production of ^{158}Er is larger than for any of the neighbouring Er nuclei. The γ-transitions within the ^{158}Er gsb are labelled in Fig. 1. The nuclei ^{159}Er and ^{160}Er are also produced with significant intensity and their γ-transitions are marked accordingly in the diagram.

Information as to which γ-transitions belong to the ^{158}Er gsb was obtained from the $\gamma\gamma$-coincidence data. In Fig. 2 two background-corrected coincidence spectra are shown. In the upper portion, a gate has been set on the $2^+ \to 0^+$ transition. In addition to the previously known rotational transitions up to the $12^+ \to 10^+$ transition, three new less intense γ-peaks at 510.0, 472.8 and 566.3 keV were observed to be in coincidence. These lines were assigned respectively as the $14^+ \to 12^+$, $16^+ \to 14^+$ and $18^+ \to 16^+$ transitions within the ^{158}Er gsb from the intensity arguments outlined above. Coincidence gates have also been placed on all transitions in the gsb, including these three new ones. From the resulting individual coincidence spectra it could be verified that

24 Draper, J. E., Lieder, R. M.: Nucl. Phys. A **141**, 211 (1970).
25 Ward, D., Stephens, F. S., Newton, J. O.: Phys. Rev. Letters **19**, 1247 (1967).
26 Nordhagen, R., Goldring, G., Diamond, R. M., Nakai, K., Stephens, F. S.: Nucl. Phys. A **142**, 577 (1970).

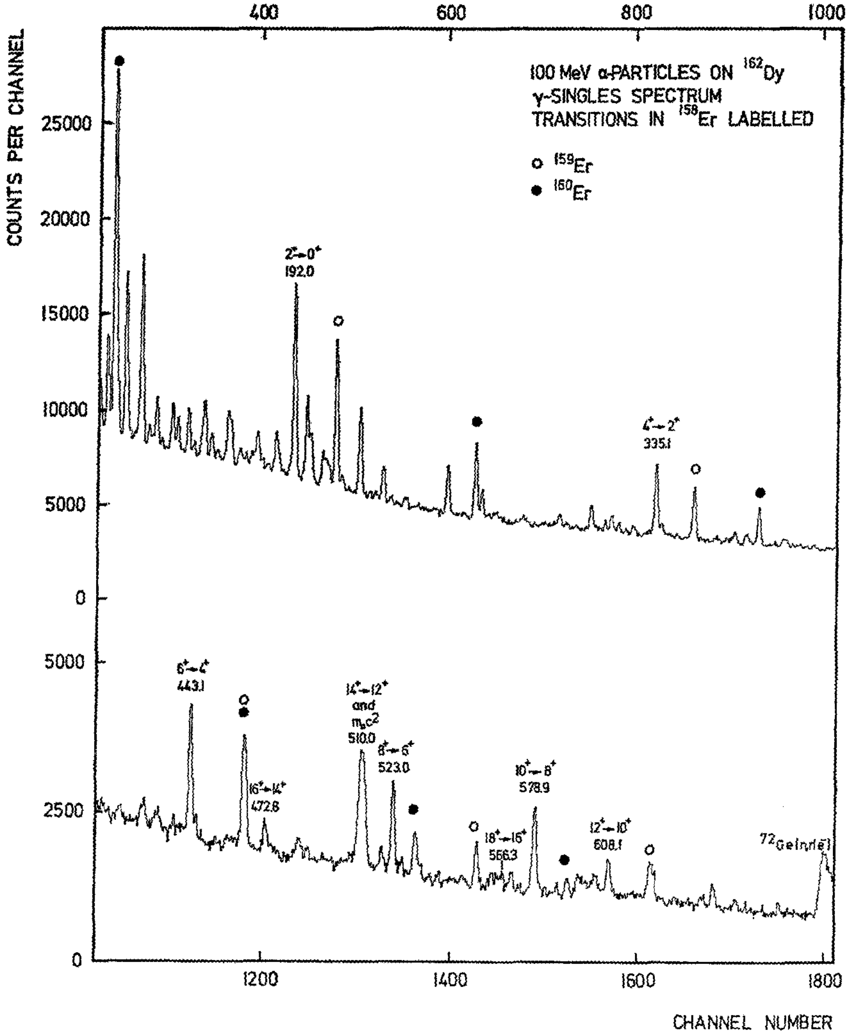

Fig. 1. A γ-singles spectrum of the reaction ^{162}Dy(α, $xn\gamma$) taken at $E_\alpha = 100$ MeV with a 6 cm^3 Ge(Li) detector. The γ-transitions belonging to the ^{158}Er gsb are labelled according to assignments made in the present study. Peaks associated with ^{159}Er and ^{160}Er are marked accordingly

these new transitions definitely belong to the gsb, and that the assignments made are consistent. In the lower portion of Fig. 2, the spectrum coincident with the $16^+ \to 14^+$ transition is shown. Paying proper regard to coincidence efficiency, within statistical errors, all transitions following this gating transition have constant intensity whereas the $18^+ \to 16^+$

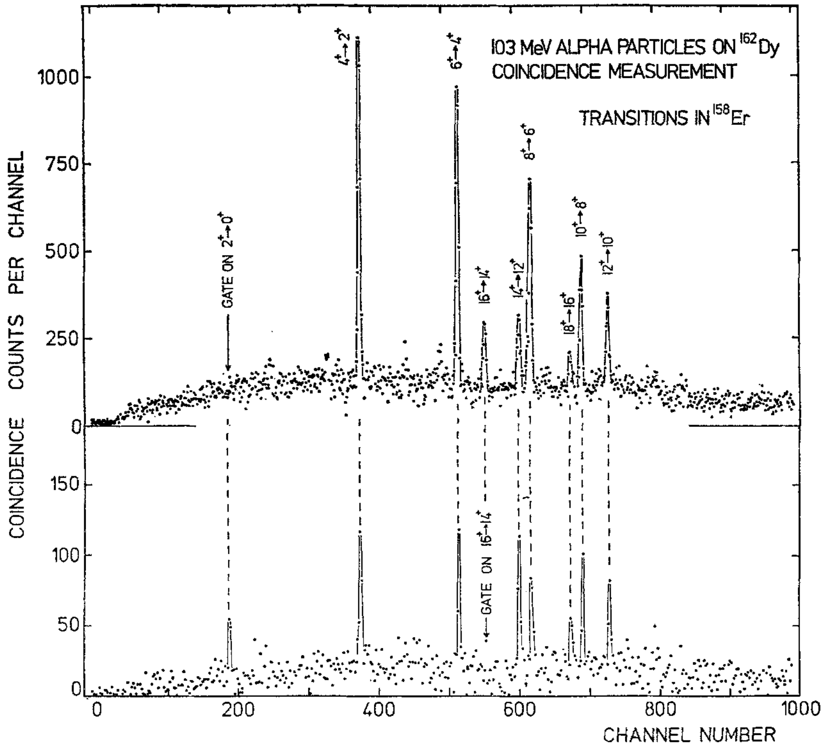

Fig. 2. Background-corrected $\gamma\gamma$-coincidence spectra gated with the $2^+\to0^+$ and $16^+\to14^+$ transitions in ^{158}Er. In comparison with the γ-singles efficiency the coincidence efficiency here gradually reduces with energy in the range of channel numbers $800\to250$ and drops off rapidly below channel 250. In the lower spectrum every two channels are summed to improve statistics

transition has reduced intensity. This supports in view of the previous arguments the sequential ordering of the transitions within the gsb.

Angular distribution measurements provided further support for these assignments in ^{158}Er. The relevant γ-spectra, taken with the high resolution 0.7 cm^3 Ge(Li) detector, were measured in time relationship with the cyclotron beam bursts. Only prompt γ-spectra were accepted in the subsequent off-line analysis of these data. In this way the radioactive γ-peaks were reduced, thereby improving spectrum quality. The results of the angular distribution measurements for all gsb transitions are shown in Fig. 3. Because the 0.7 cm^3 detector has low efficiency, measurements were limited to the three angles 90°, 120° and 150°. The solid lines are fits of the angular distribution function

$$W(\theta)=A_0+A_2\,P_2(\cos\theta)+A_4\,P_4(\cos\theta)$$

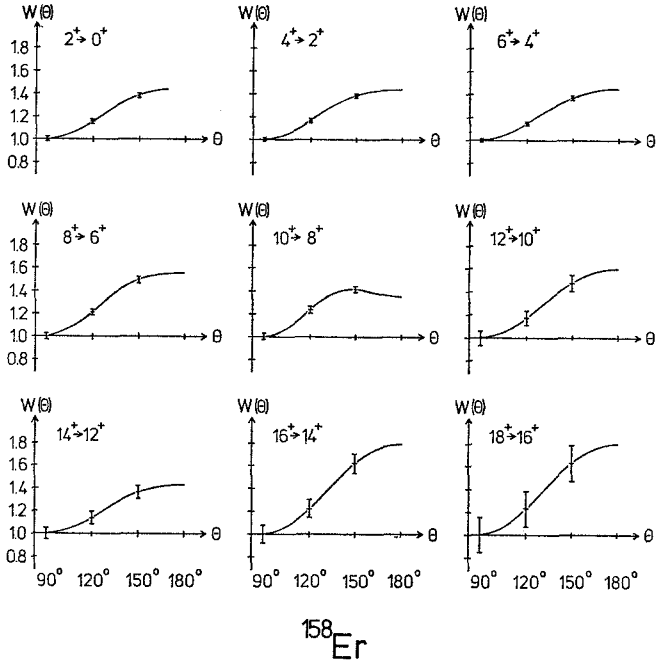

Fig. 3. Angular distribution measurements for the gsb transitions in ^{158}Er. The solid curves are fits to the experimental data points of the angular distribution function $W(\theta)$ normalised to $W(90°)$

to the experimental points normalised to $W(90°)$. As can be seen, all these curves exhibit a large positive anisotropy which is characteristic for stretched $E2$ transitions. Furthermore the magnitude of the anisotropy decreases gradually as the γ-cascade proceeds down the gsb until the 6^+ state is reached. This feature can be explained by sidefeeding arguments. Exceptions from this general trend are the angular distributions of the $10^+ \to 8^+$ and $14^+ \to 12^+$ transitions, whose peaks in the γ-spectrum are contaminated, as can be observed in Fig. 1. The final normalised Legendre coefficients together with the energies of the γ-transitions are given in Table 2.

To obtain the relative intensity of the gsb transitions the prompt γ-spectrum taken at 150° in the angular distribution measurements was used. The intensity of the $10^+ \to 8^+$ transition was determined after subtracting out a contaminating component due to the $12^+ \to 10^+$ transition in ^{160}Er. The intensity of the $14^+ \to 12^+$ transition at 510.0 keV could be corrected for the contaminating annihilation peak which in this spectrum was reduced by a factor of five in comparison with the

Table 2. Energies in keV and angular distribution coefficients of rotational transitions in ^{158}Er

Transition	E^a	A_2/A_0	A_4/A_0
$2^+ \to 0^+$	192.0	0.27 ± 0.02	-0.05 ± 0.04
$4^+ \to 2^+$	335.1	0.27 ± 0.02	-0.06 ± 0.02
$6^+ \to 4^+$	443.1	0.27 ± 0.02	-0.04 ± 0.03
$8^+ \to 6^+$	523.0	0.33 ± 0.03	-0.07 ± 0.05
$10^+ \to 8^+$	578.9	0.25 ± 0.03^b	-0.15 ± 0.05^b
$12^+ \to 10^+$	608.1	0.34 ± 0.08	-0.02 ± 0.13
$14^+ \to 12^+$	510.0	0.26 ± 0.07^c	-0.04 ± 0.11^c
$16^+ \to 14^+$	472.8	0.42 ± 0.09	-0.03 ± 0.15
$18^+ \to 16^+$	566.3	0.43 ± 0.17	-0.03 ± 0.28

[a] Energies determined to ± 0.3 keV.
[b] Contains contribution of a contaminating line.
[c] Contains contribution of isotropic annihilation radiation.

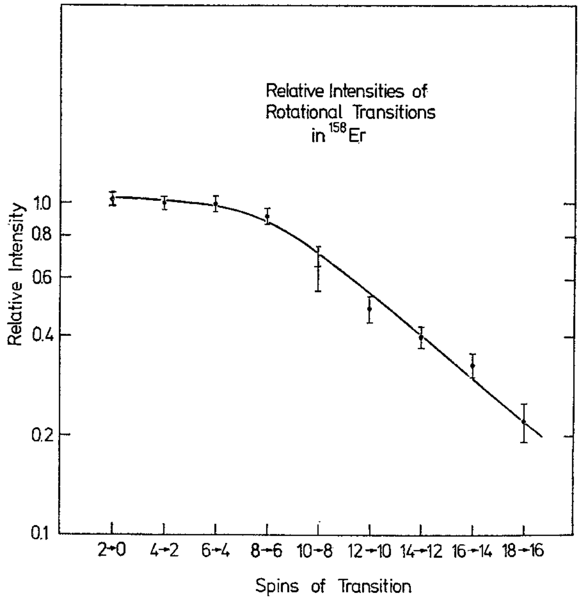

Fig. 4. Relative intensities of gsb transitions in ^{158}Er as a function of spin, as derived from a γ-singles spectrum taken at 150° with respect to the beam axis. A planar 0.7 cm^3 Ge(Li) detector was used to measure the γ-spectrum

singles spectrum shown in Fig. 1. In Fig. 4 the relative intensity of the gsb transitions, corrected for internal conversion, is plotted as a function of the spins of the gsb transitions. The relative intensities of the transitions progressively increase from $18^+ \to 16^+$ down to $8^+ \to 6^+$ after

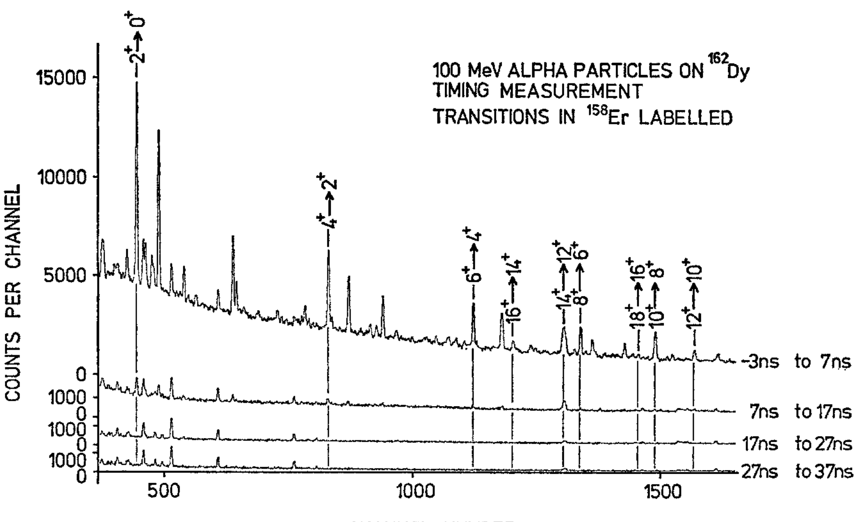

Fig. 5. Two-parameter γ-spectrum for the reaction $^{162}Dy(\alpha, xn\gamma)$. The counting rate is plotted versus pulse height for four different time bands. The width and location of the time bands are indicated. The beam burst is in the time band labelled −3 to 7 ns. The $14^+ \to 12^+$ transition is contaminated by annihilation radiation

which point the relative intensities are constant within statistical uncertainty. This corresponds to no side-feeding to the first two excited states, and possibly only a small amount to the third excited state. That all the points lie on a smooth curve indicates that the spin assignments are the most probable.

To prove that all the gsb transitions in ^{158}Er are in no way associated with the deexcitation of isomeric states, γ-spectra were measured at different time intervals within the 45 ns duty cycle. The resultant two-parameter spectrum is shown in Fig. 5. It can be seen that the relevant γ-transitions decay within the prompt peak. However the time dependence of the $14^+ \to 12^+$ transition could not be determined since it is superimposed by the annihilation radiation peak. It was concluded that no isomeric state with a halflife larger than 2 ns is associated with the gsb.

3.2. The Nucleus ^{160}Er

Prior to this investigation information on the gsb up to the 12^+ state in ^{160}Er was available in the literature[22,25,26]. Similar results to those reported here have been recently obtained by A. Johnson and coworkers using the (^{16}O, $xn\gamma$) reaction[27].

27 Johnson, A., Ryde, H., Hjorth, S. A.: Contribution to the Symposium on High Spin Nuclear States and Related Phenomena, Stockholm 1972.

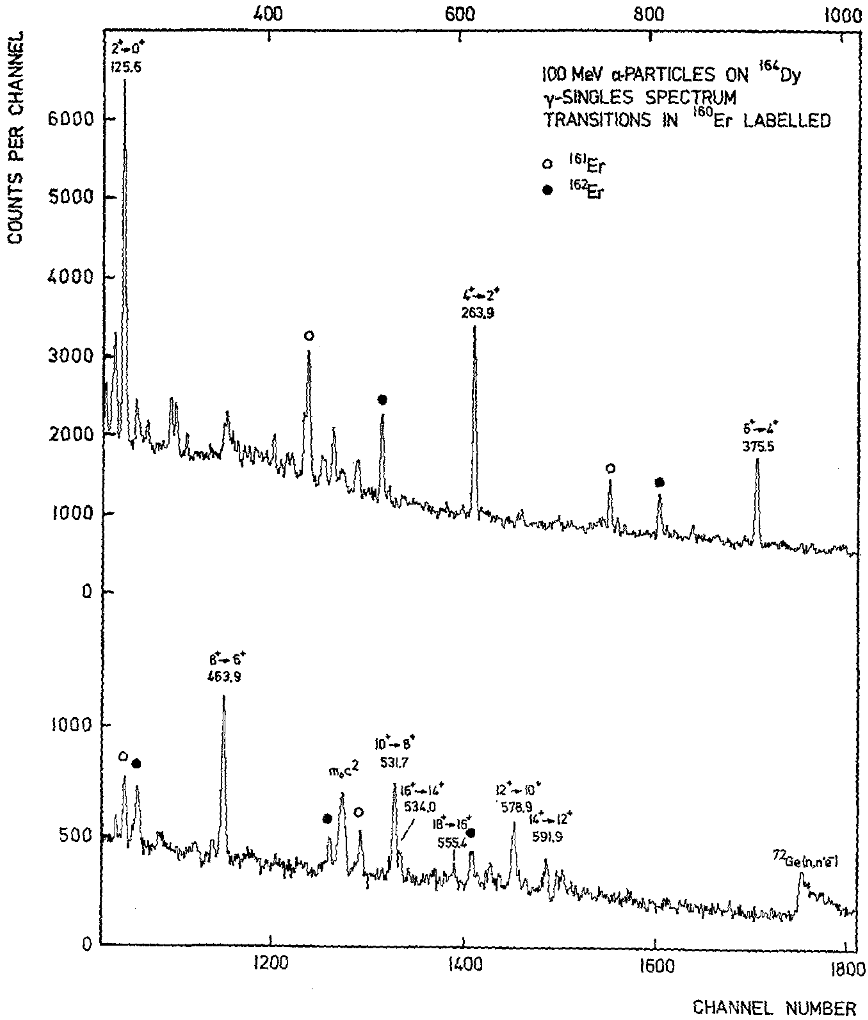

Fig. 6. A γ-singles spectrum of the reaction $^{164}Dy(\alpha, xn\gamma)$ taken at $E_\alpha = 100$ MeV. The γ-transitions belonging to the ^{160}Er gsb are labelled according to assignments made in the present study. Peaks associated with ^{161}Er and ^{162}Er are marked accordingly

In Fig. 6 a γ-singles spectrum is shown for the reaction $^{164}Dy(\alpha, xn\gamma)$ for $E_\alpha = 100$ MeV. In this case the yield of ^{160}Er is considerably larger than for the neighbouring isotopes ^{161}Er and ^{162}Er, as can be seen in the figure. The γ-transitions in these three nuclei have been identified and labelled.

In the $\gamma\gamma$-coincidence data, gates were set on all known gsb γ-transitions as well as on all other interesting γ-peaks which could potentially

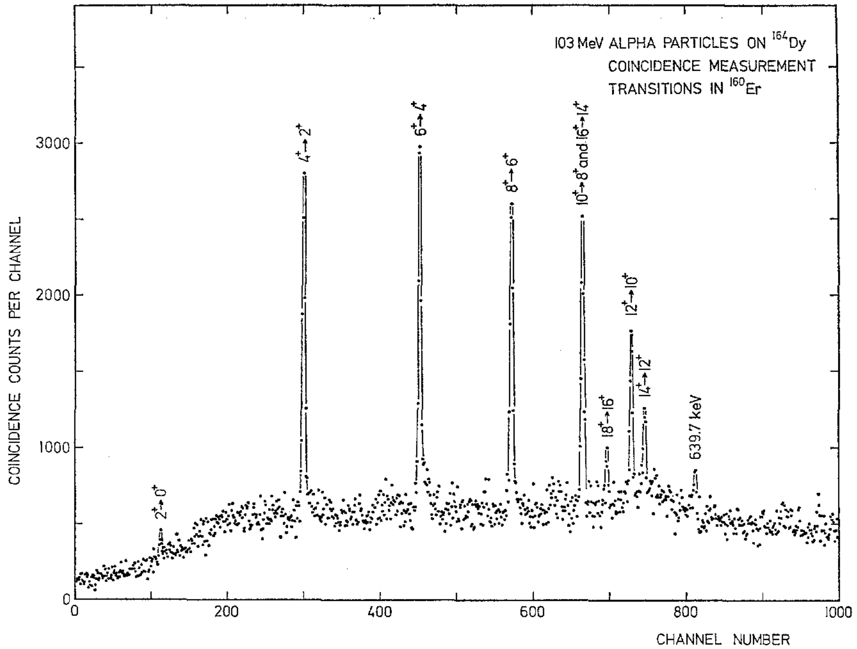

Fig. 7. Sum of nine background-corrected $\gamma\gamma$-coincidence spectra resulting from gates placed on each individual gsb transition up to the $18^+ \rightarrow 16^+$ transition in ^{160}Er. The 639.7 keV transition does not belong to the gsb

belong to the gsb. From the corresponding coincidence spectra three new coincident transitions of energies 591.9, 534.0, and 555.4 keV were discovered, and from similar arguments as given above in the case of ^{158}Er they were assigned as the $14^+ \rightarrow 12^+$, $16^+ \rightarrow 14^+$, and $18^+ \rightarrow 16^+$ transitions within the ^{160}Er gsb cascade. Since the older experimental configuration mentioned in Section 2 was used to obtain the coincidence data for ^{160}Er, subtraction of the higher backgrounds produced resultant coincidence spectra whose statistical quality was somewhat poorer than in the ^{158}Er case. However summing of background-corrected coincidence spectra[10] associated with gates set on all nine cascade γ-transitions up to the 18^+ state served to maximise statistics and the resultant summed coincidence spectrum is displayed in Fig. 7. It was established from these coincidence measurements that the line at $\sim$531 keV known previously as the $10^+ \rightarrow 8^+$ transition was a doublet, the other component being identified as the $16^+ \rightarrow 14^+$ transition. The two transitions are much better resolved in the high resolution γ-singles spectrum in Fig. 6.

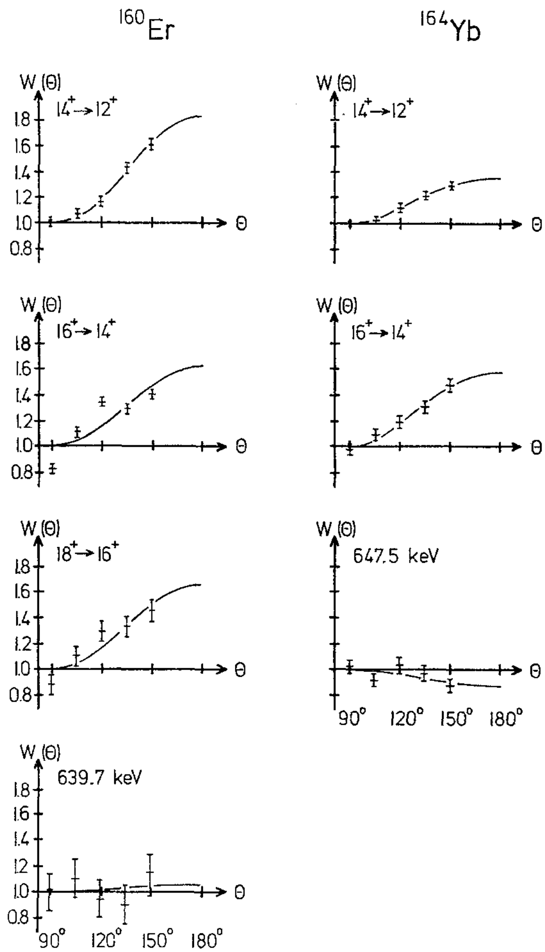

Fig. 8. Angular distribution measurements for the top three gsb transitions in ^{160}Er and the top two gsb transitions in ^{164}Yb. Angular distributions for the anomalous coincident γ-transitions at 639.7 keV in ^{160}Er and at 647.5 keV in ^{164}Yb are also displayed. The solid curves are fits to the experimental data points of the angular distribution function $W(\theta)$ normalised to $W(90°)$

The angular distributions of all gsb transitions in ^{160}Er showed the strong anisotropy which is typical for a stretched $E2$ cascade. The angular distribution patterns for the three new gsb transitions are shown in Fig. 8. In Table 3 the Legendre coefficients and γ-energies of all gsb transitions are presented.

The relative transition intensity in the gsb of ^{160}Er plotted as a function of spin is shown in Fig. 9 giving added support for the ordering of

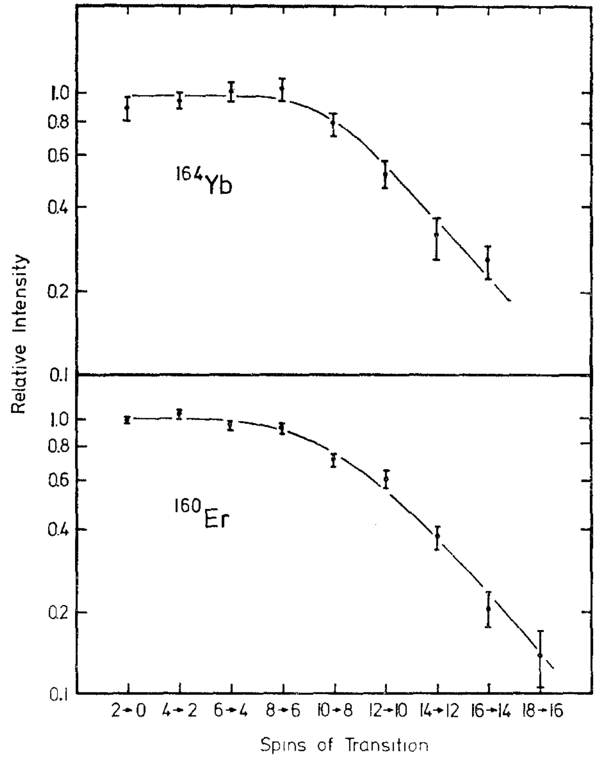

Fig. 9. Relative intensities of gsb transitions as a function of spin in ^{164}Yb and ^{160}Er, as derived from γ-singles spectra taken at 135° with respect to the beam axis. These intensities were obtained using a planar 6 cm^3 Ge(Li) detector

Table 3. Energies in keV and angular distribution coefficients of rotational transitions in ^{160}Er. The transition at 639.7 keV does not belong to the gsb and is discussed in Section 4

Transition	E^{a}	A_2/A_0	A_4/A_0
$2^+ \to 0^+$	125.6	0.24 ± 0.01	-0.07 ± 0.02
$4^+ \to 2^+$	263.9	0.28 ± 0.01	-0.05 ± 0.02
$6^+ \to 4^+$	375.5	0.30 ± 0.01	-0.07 ± 0.02
$8^+ \to 6^+$	463.9	0.30 ± 0.01	-0.10 ± 0.02
$10^+ \to 8^+$	531.7	0.39 ± 0.02	-0.00 ± 0.03
$12^+ \to 10^+$	578.9	0.30 ± 0.02^{b}	-0.07 ± 0.04
$14^+ \to 12^+$	591.9	0.43 ± 0.05	-0.02 ± 0.07
$16^+ \to 14^+$	534.0	0.34 ± 0.03^{c}	
$18^+ \to 16^+$	555.4	0.36 ± 0.06^{c}	
	639.7	0.02 ± 0.16^{c}	

[a] Energies determined to ± 0.3 keV.

[b] Contains contribution of a contaminating line.

[c] Fit restricted to A_2/A_0 only because of weak nature of peak.

the gsb transitions. The timing spectra indicated the absence of any isomeric states feeding into the gsb.

In this nucleus a γ-transition of energy 639.7 keV with interesting features was observed. This γ-transition (labelled in Fig. 7) appears to fulfil all coincidence and intensity requirements of a $20^+ \rightarrow 18^+$ transition. However the angular distribution of this γ-ray shown in Fig. 8 does not exhibit the anisotropy required by a stretched $E2$ transition. The angular distribution coefficient A_2/A_0 is included in Table 3. This γ-transition is discussed in Section 4.

3.3. The Nucleus ^{164}Yb

The ^{164}Yb gsb is reliably known up to 12^+ from the work of Stephens *et al.*[28].

In Fig. 10 a γ-singles spectrum of the reaction $^{168}Er(\alpha, xn\gamma)$ for $E_\alpha = 100$ MeV is shown where transitions in ^{164}Yb, which has the largest yield, and in the neighbouring nucleus ^{166}Yb are marked. A summed coincidence spectrum is shown in Fig. 11 which was obtained similarly as for the ^{160}Er case (cf. Section 3.2). From systematic study of each individual coincidence γ-spectrum, the existence of two new gsb γ-transitions at 569.7 and 490.0 keV were established and assigned as $14^+ \rightarrow 12^+$ and $16^+ \rightarrow 14^+$ members respectively. The γ-intensities as a function of spin are shown in Fig. 9.

In Table 4 angular distribution coefficients for all transitions are given together with the energies. These coefficients establish the stretched $E2$ character of the transitions. The angular distributions for the two new transitions are shown in Fig. 8. All these γ-transitions have been found to be prompt.

Table 4. Energies in keV and angular distribution coefficients of rotational transitions in ^{164}Yb. The transition at 647.5 keV does not belong to the gsb and is discussed in Section 4

Transition	E^a	A_2/A_0	A_4/A_0
$2^+ \rightarrow 0^+$	123.3	0.19 ± 0.02	-0.11 ± 0.03
$4^+ \rightarrow 2^+$	262.4	0.29 ± 0.01	-0.03 ± 0.02
$6^+ \rightarrow 4^+$	374.7	0.30 ± 0.02	-0.05 ± 0.02
$8^+ \rightarrow 6^+$	463.0	0.30 ± 0.02	-0.08 ± 0.03
$10^+ \rightarrow 8^+$	530.9	0.39 ± 0.02	-0.06 ± 0.03
$12^+ \rightarrow 10^+$	576.9	0.35 ± 0.04	0.00 ± 0.06
$14^+ \rightarrow 12^+$	569.7	0.22 ± 0.03^b	-0.03 ± 0.04^b
$16^+ \rightarrow 14^+$	490.0	0.33 ± 0.05	-0.03 ± 0.07
	647.5	0.08 ± 0.06^c	

[a] Energies determined to ± 0.3 keV.
[b] Contains contribution of contaminating lines of ^{207}Pb and ^{166}Yb.
[c] Fit restricted to A_2/A_0 only because of weak nature of peak.

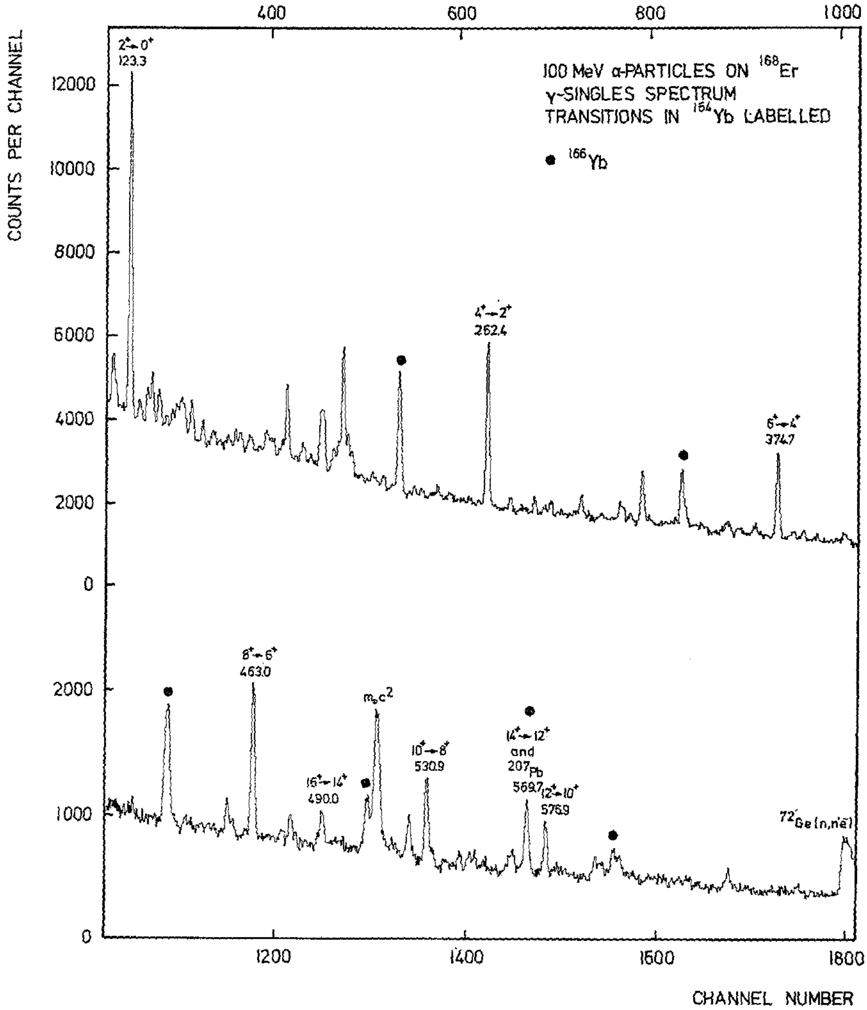

Fig. 10. A γ-singles spectrum of the reaction $^{168}Er(\alpha, xn\gamma)$ taken at $E_\alpha = 100$ MeV. The γ-transitions belonging to the ^{164}Yb gsb are labelled according to assignments made in the present study. Peaks associated with the nucleus ^{166}Yb are also marked

In the study of this nucleus a γ-ray of energy 647.5 keV was found in coincidence with all gsb γ-transitions. As can be seen from its angular distribution shown in Fig. 8, and the A_2/A_0 coefficient in Table 4, this transition does not show stretched $E2$ character but displays a behaviour similar to that of the 639.7 keV transition in ^{160}Er. This transition is discussed in Section 4.

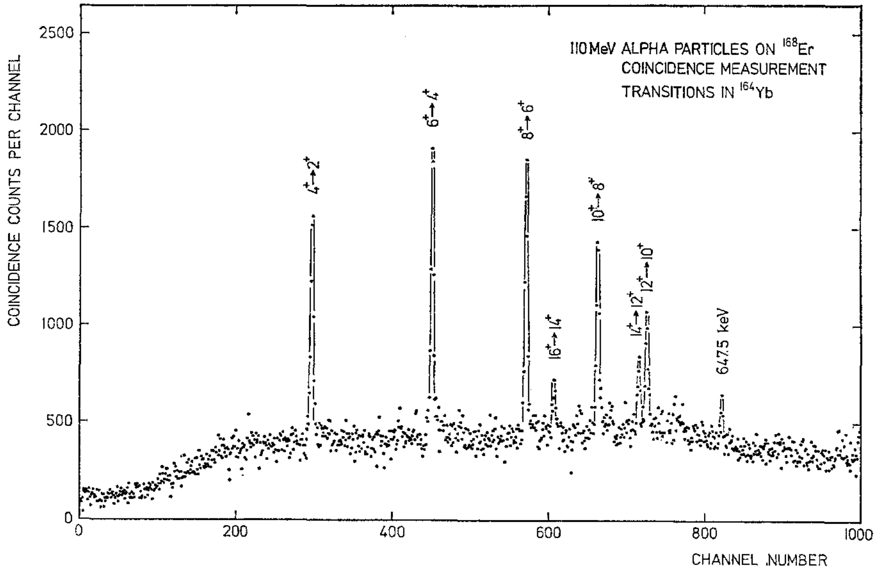

Fig. 11. Sum of eight background-corrected $\gamma\gamma$-coincidence spectra resulting from gates placed on each individual gsb transition up to the $16^+ \to 14^+$ transition in ^{164}Yb. The 647.5 keV transition does not belong to the gsb

3.4. *The Nucleus ^{166}Yb*

The ^{166}Yb gsb is known with reliability up to the 12^+ state from previous electron conversion work[28].

A singles γ-spectrum of the reaction ^{170}Er$(\alpha, xn\gamma)$ for $E_\alpha = 100$ MeV is shown in Fig. 12. In addition to the gsb transitions in ^{166}Yb γ-transitions of the neighbouring nucleus ^{168}Yb are marked. The coincidence spectra were taken with the improved set-up and have the same quality as for ^{158}Er. In Fig. 13 two background-corrected coincidence spectra are presented gated with the $10^+ \to 8^+$ and the $12^+ \to 10^+$ transitions. From consideration of all coincidence spectra new transitions up to $20^+ \to 18^+$ have been identified. From the upper spectrum where a gate was set on the $10^+ \to 8^+$ peak at ≈ 508 keV it was concluded that this peak is double since this was the only coincidence spectrum in which the gating peak did not vanish. Furthermore in the lower spectrum coincident with the $12^+ \to 10^+$ transition, this ≈ 508 keV peak is more intense than all other transitions following the $12^+ \to 10^+$ transition. Fig. 14 shows γ-intensities plotted against the spin value of the higher transitions derived from these coincidence spectra under the assumption

28 Stephens, F. S., Lark, N. L., Diamond, R. M.: Nucl. Phys. **63**, 82 (1965).

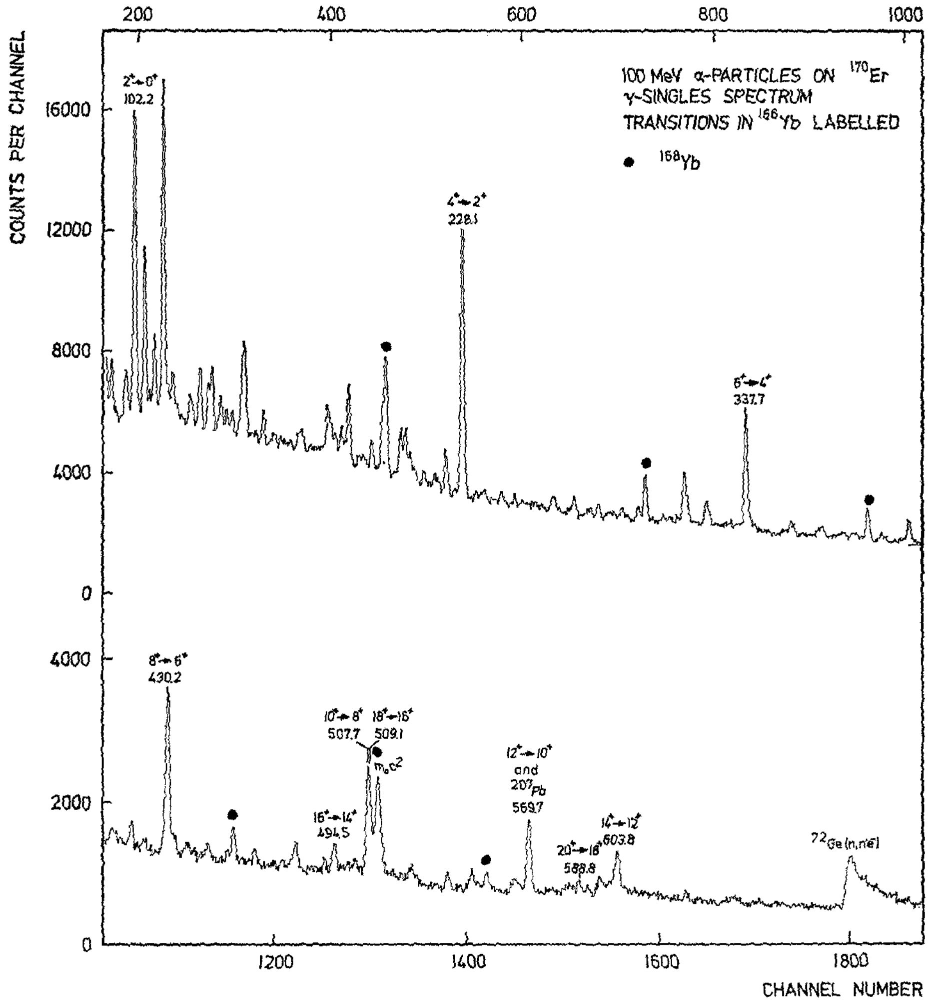

Fig. 12. A γ-singles spectrum of the reaction ^{170}Er(α, *xn*γ) taken at $E_\alpha = 100$ MeV. The γ-transitions belonging to the ^{166}Yb gsb are labelled according to assignments made in the present study. Peaks associated with the nucleus ^{168}Yb are also marked

that the second component of the doublet is the $18^+ \rightarrow 16^+$ transition. The monotonic fall-off and the fact that in both cases the intensities are identical within statistical errors indicate that the proposed assignments are the most probable.

Angular distributions measured with the 0.7 cm^3 Ge(Li) spectrometer are presented in Fig. 15. The patterns support *E*2 character and

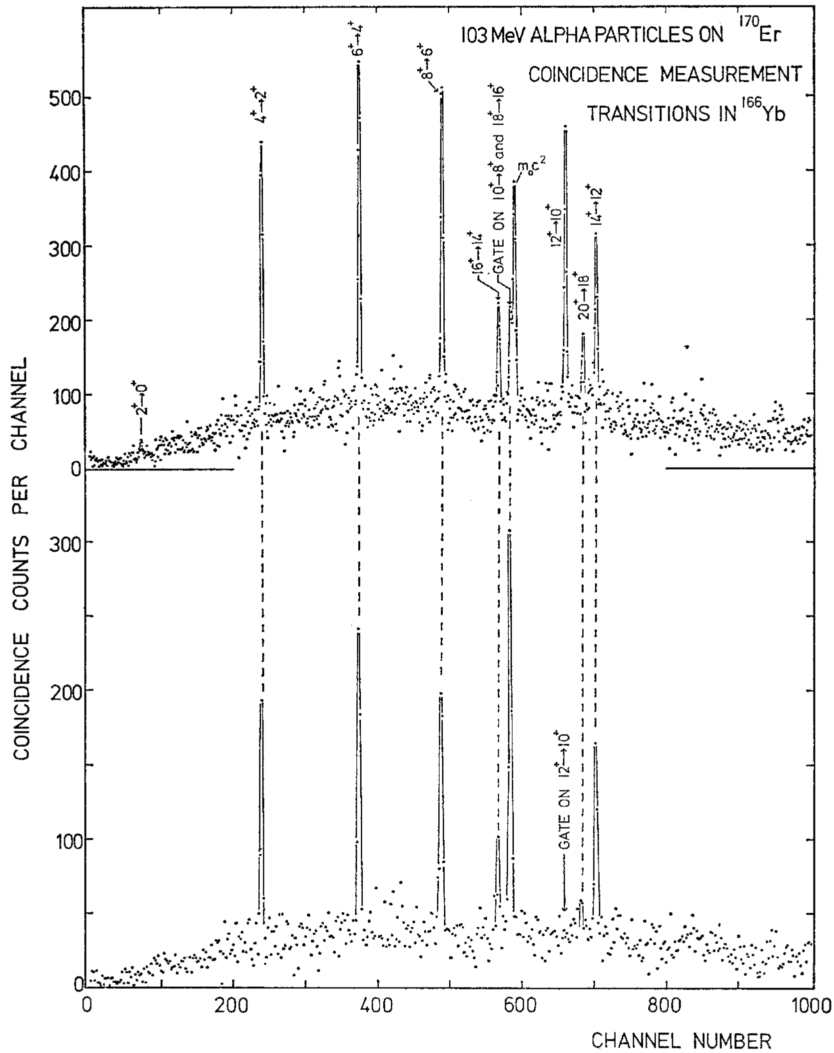

Fig. 13. Background-corrected $\gamma\gamma$-coincidence spectra gated on the doublet comprising the $10^+ \to 8^+$ and $16^+ \to 14^+$ transitions, and on the $12^+ \to 10^+$ transition, in ^{166}Yb. The annihilation radiation peak appears in the upper spectrum since the $10^+ \to 8^+$ peak is not completely resolved from the 511 keV line. For further explanations see caption to Fig. 2

the gradual fall-off in anisotropy with decreasing spin is clearly evident. The Legendre coefficients and the γ-transition energies are given in Table 5.

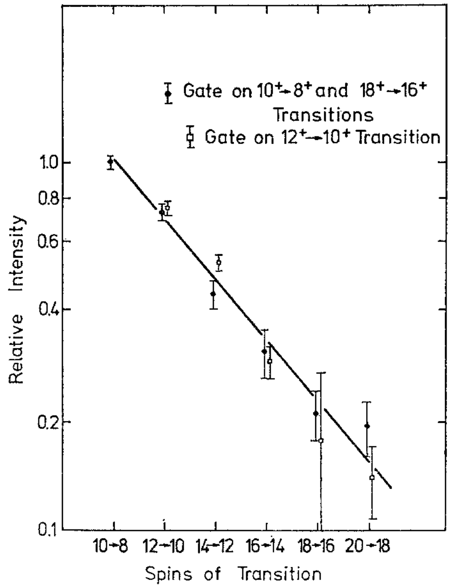

Fig. 14. Relative intensities of rotational transitions in ^{166}Yb as a function of spin derived from the coincidence spectra in Fig. 13

Table 5. Energies in keV and angular distribution coefficients of rotational transitions in ^{166}Yb

Transition	E^a	A_2/A_0	A_4/A_0
$2^+ \to 0^+$	102.2	0.25 ± 0.03	-0.11 ± 0.04
$4^+ \to 2^+$	228.1	0.30 ± 0.01	-0.03 ± 0.02
$6^+ \to 4^+$	337.7	0.30 ± 0.01	-0.03 ± 0.02
$8^+ \to 6^+$	430.2	0.33 ± 0.02	-0.05 ± 0.03
$10^+ \to 8^+$	507.7	0.35 ± 0.02	-0.10 ± 0.04
$12^+ \to 10^+$	569.7	0.32 ± 0.03^b	-0.05 ± 0.05
$14^+ \to 12^+$	603.8	0.34 ± 0.05	-0.05 ± 0.09
$16^+ \to 14^+$	494.5	0.41 ± 0.09	-0.03 ± 0.14
$18^+ \to 16^+$	509.1	$-^c$	$-^c$
$20^+ \to 18^+$	588.8	0.44 ± 0.15	-0.04 ± 0.25

[a] Energies determined to ± 0.3 keV.
[b] Contaminated by the 569.7 keV transition in ^{207}Pb.
[c] Angular distribution not available for the $18^+ \to 16^+$ transition.

Fig. 16 shows time spectra for the $8^+ \to 6^+$ and higher transitions. These were obtained by setting gates on the appropriate γ-peaks in the two dimensional time vs. energy spectrum. As can be shown all tran-

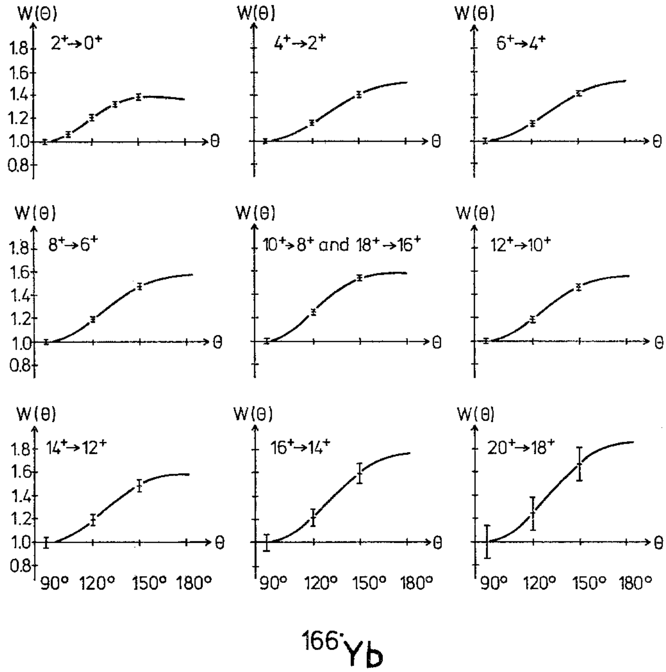

Fig. 15. Angular distribution measurements for the gsb transitions in ^{166}Yb. The solid curves are fits to the experimental data points of the angular distribution function $W(\theta)$ normalised to $W(90°)$

sitions are prompt and an upper limit on the halflife of any of these transitions was estimated to be 2 ns.

3.5. *The Nucleus* ^{168}*Hf*

Transitions up to the 12^+ state in ^{168}Hf have previously been identified by Stephens *et al.*[28].

A γ-singles spectrum of the reaction ^{172}Yb$(\alpha, xn\gamma)$ at $E_\alpha = 100$ MeV is shown in Fig. 17. Transitions identified with the gsb in ^{168}Hf are labelled, as are peaks attributed to ^{170}Hf.

As in the cases of ^{160}Er and ^{164}Yb, a summed coincidence spectrum was constructed and is shown in Fig. 18. A new transition at energy 551.6 keV was identified as the $14^+ \to 12^+$ gsb transition. In addition in the best resolved coincidence spectra two more γ-peaks appear at 453 and 460 keV on each side of the $8^+ \to 6^+$ γ-transition at 456.6 keV. In Fig. 18 the 460 keV γ-peak can be clearly seen. The individual coincidence spectra do not give completely conclusive information as to the origin of

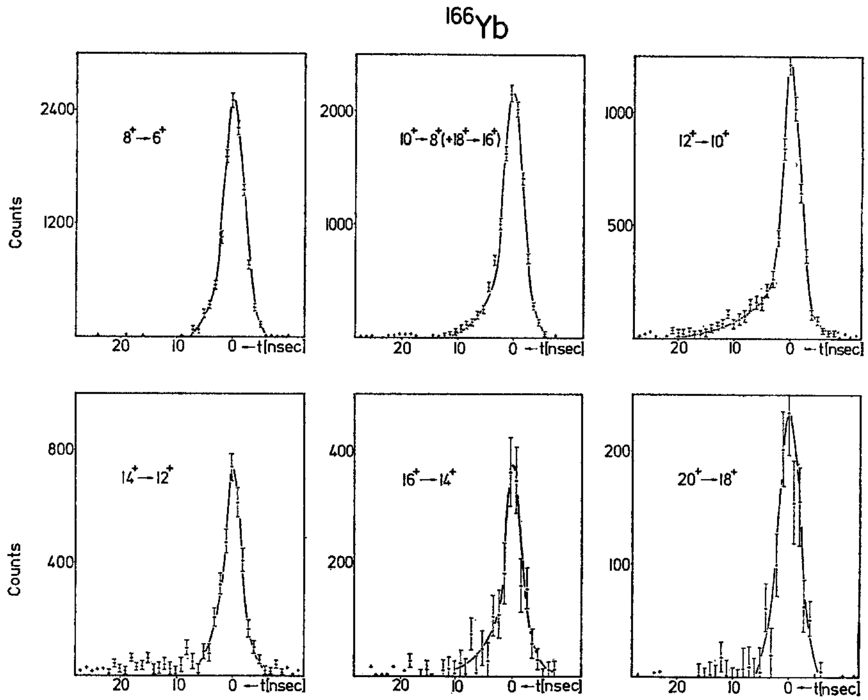

Fig. 16. Time spectra of the higher gsb transitions in ^{166}Yb. The prompt peaks have the instrumental shape, i. e. 6 ns FWHM and slopes of 2 ns. In the case of the $12^+ \to 10^+$ transition, a background component is not completely subtracted out

Table 6. Energies in keV and angular distribution coefficients of rotational transitions in ^{168}Hf

Transition	E^a	A_2/A_0	A_4/A_0
$2^+ \to 0^+$	123.7	0.27 ± 0.02	-0.01 ± 0.02
$4^+ \to 2^+$	261.5	0.31 ± 0.01	0.00 ± 0.02
$6^+ \to 4^+$	371.2	0.29 ± 0.02	-0.02 ± 0.02
$8^+ \to 6^+$	456.6	0.34 ± 0.02	0.05 ± 0.03
$10^+ \to 8^+$	522.0	0.34 ± 0.03	0.02 ± 0.04
$12^+ \to 10^+$	569.8	0.30 ± 0.02^b	0.05 ± 0.03
$14^+ \to 12^+$	551.6	0.33 ± 0.05^c	0.04 ± 0.07

[a] Energies are determined to ± 0.3 keV.
[b] Contaminated by the 569.7 keV transition in ^{207}Pb.
[c] Superimposed by the $12^+ \to 10^+$ transition in ^{170}Hf.

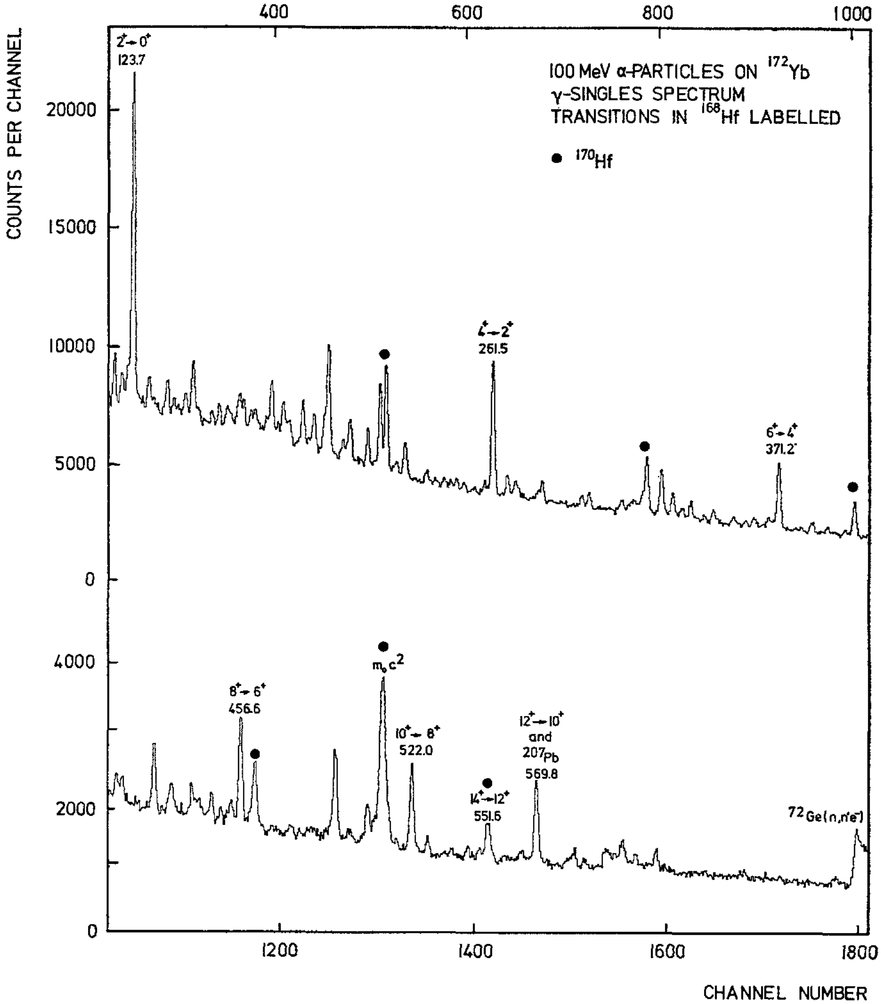

Fig. 17. A γ-singles spectrum of the reaction ^{172}Yb(α, $xn\gamma$) taken at $E_\alpha = 100$ MeV. The γ-transitions belonging to the ^{168}Hf gsb are labelled according to assignments made in the present study. Peaks associated with ^{170}Hf are marked accordingly

these two γ-rays. However one of these γ-peaks is believed to be the $16^+ \to 14^+$ transition. Much better coincidence spectra are needed to completely resolve this problem.

The angular distributions of all the gsb transitions have stretched $E2$ character. The transitions come promptly with respect to the beam pulses. The Legendre coefficients and the energies are given in Table 6.

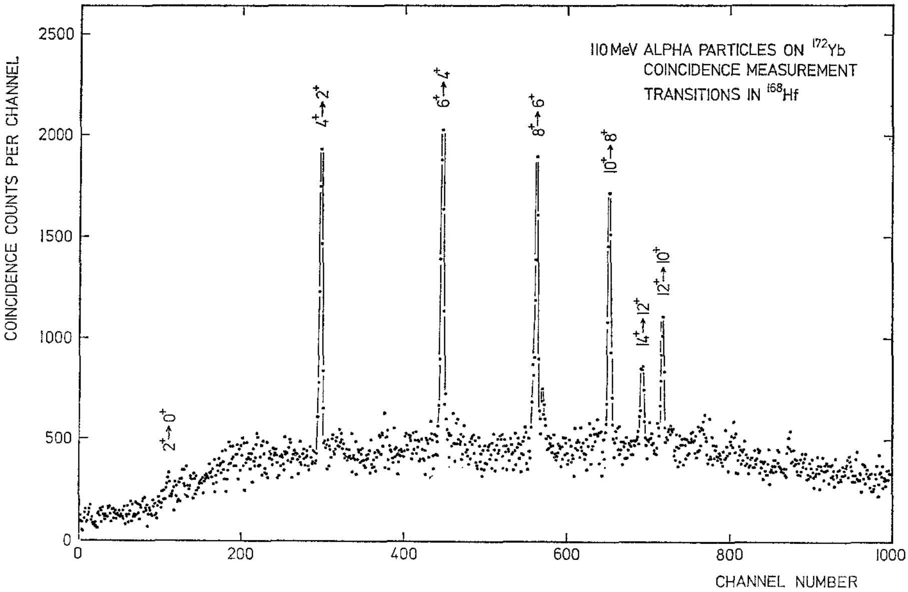

Fig. 18. Sum of seven background-corrected $\gamma\gamma$-coincidence spectra resulting from gates placed on each individual gsb transition up to the $14^+ \to 12^+$ transition in ^{168}Hf

4. Anomalous Coincident γ-Transitions

In Section 3 the existence of two unusual coincident γ-rays, one at 639.7 keV in ^{160}Er and the other at 647.5 keV in ^{164}Yb, was reported. It is the aim of this section to discuss the nature of these two transitions.

Both these transitions which are in coincidence with all known cascade γ-transitions in their respective ground state bands seem to feed into the highest known level of the gsb, namely the 18^+ state in ^{160}Er and the 16^+ state in ^{164}Yb. This is suggested by comparing their intensities with the intensities of the highest known gsb transitions. In ^{160}Er the ratio of the γ-intensity of the 639.7 keV transition to the $18^+ \to 16^+$ transition is 0.6 ± 0.2 and in ^{164}Yb the ratio of the 647.5 keV to the $16^+ \to 14^+$ transition is 1.0 ± 0.2. An additional feature is that both γ-rays come promptly with respect to the beam bursts.

From consideration of the angular distribution coefficient A_2/A_0 (given in Tables 3 and 4) for these two transitions it can be seen that they are inconsistent with stretched $E2$ multipolarity. The experimental A_2/A_0 coefficient for the 647.5 keV transition in ^{164}Yb was compared with theoretical A_2/A_0 coefficients for the sequences $I_i(L, L')\, I_f = 17(1,2)16$, $16(1,2)16$ and $15(1,2)16$. Here I_i and I_f denote initial and final spins of states connected by a γ-transition of mixed dipole and quadrupole multipolarity. Under the plausible assumption that $|A_4/A_0| < 0.3$ inferred from the experimental angular distributions, there is no solution for the sequence 16(1, 2) 16. However for the sequences 17 (1, 2) 16 and 15(1, 2)16, solutions are just admissible for $Q=\delta^2/1+\delta^2=0.005 \pm 0.005$ and for $Q=0.97 \pm 0.03$, where δ is the dipole-quadrupole mixing ratio. This means that the transition probably has either pure dipole or pure unstretched quadrupole character. Similar conclusions were also drawn for the less intense 639.7 keV γ-transition in ^{160}Er.

The occurence of a γ-transition at 652.9 keV in ^{162}Er whose angular distribution was also consistent with dipole multipolarity was recently reported verbally by Sunyar and coworkers[29].

If the above γ-rays were of dipole nature, it would be interesting to establish whether the γ-rays have $M1$ or $E1$ character. If the γ-ray is $M1$ (no parity change), the initial state emitting this γ-ray could be a state made up from configuration mixing of two- or four-quasi-particle states in the $i_{13/2}$ orbital. If however the γ-ray is $E1$ and hence the parity changes, the state must have a totally different structure since it must be composed of $i_{13/2}$ orbitals plus some other negative parity orbitals, possibly the $h_{11/2}$ or $j_{15/2}$. However if the above γ-rays were unstretched quadrupole transitions, they should have $E2$ multipolarity for the following reason. Generally the feeding times are short; in ^{160}Er for instance this time is ~ 6 ps (Ref.[22]). Since the Weisskopf estimate for the halflife of a 639 keV transition of $M2$ multipolarity is 10 ns, $M2$ multipolarity is very unlikely.

5. Discussion

In order to obtain more insight into the behaviour of the above nuclei at high angular momenta, it is instructive to derive from the data given in Tables 2 through 6 how the nuclear moments of inertia depend on the rotational frequency.

The moment of inertia is defined as

$$\frac{2\theta}{\hbar^2}=\left[\frac{dE}{d(I(I+1))}\right]^{-1}$$

and the rotational frequency ω is defined as

$$\hbar\omega=\frac{dE}{d\sqrt{I(I+1)}}.$$

29 Sunyar, A. W., Cochavi, S., Kistner, O. C., der Mateosian, E., Thieberger, P.: Contribution to the Symposium on High Spin Nuclear States and Related Phenomena, Stockholm 1972.

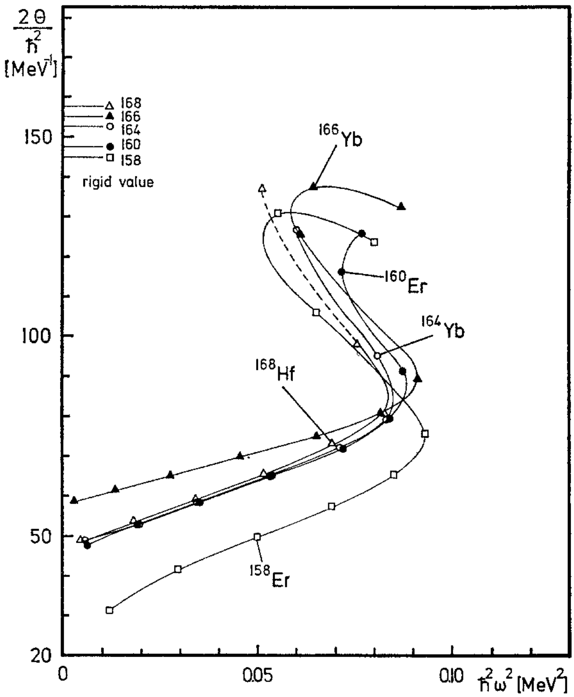

Fig. 19. Nuclear moment of inertia versus the square of the rotational frequency for the gsb in $^{158,160}Er$, $^{164,166}Yb$, and ^{168}Hf. The experimental points correspond to the different transitions within the gsb. The leftmost point of each curve corresponds to the $2^+ \rightarrow 0^+$ transition, the next one to the $4^+ \rightarrow 2^+$ transition, and so on. The experimental points are connected by curves to guide the eye

Following the procedure outlined by the Swedish group[1] plots were made of $2\theta/\hbar^2$ vs. $\hbar^2\omega^2$. These quantities were obtained by replacing the derivative with the corresponding differential quotient evaluated between the spin values I and $I-2$, and are given by

$$\frac{2\theta}{\hbar^2}=\frac{4I-2}{E_I-E_{I-2}}$$

and

$$\hbar^2\omega^2=\frac{I^2-I+1}{(2I-1)^2}[E_I-E_{I-2}]^2.$$

Here I denotes the spin of the initial state, and $[E_I-E_{I-2}]$ is the transition energy.

In Fig. 19 these plots for all five nuclei are presented. It can be seen that in all cases the moment of inertia increases monotonically up to a spin of 10^+ or 12^+ in accordance with what is expected from consideration of the VMI model[30]. However beyond this region of spin values all these five curves bend both backwards and upwards in a very dramatic manner. Here the moment of inertia increases much more rapidly from level to level than in the lower portion of the gsb.

In ^{158}Er and ^{166}Yb the curves reach a maximum at $I=16^+$ and 18^+ respectively and then bend forwards with a downward slope. At their respective maxima the moments of inertia come close to the rigid rotor values evaluated at $\omega=0$. The maxima values are 130 MeV^{-1} in ^{158}Er, and 140 MeV^{-1} in ^{166}Yb, which are about 90% of the rigid rotor values. The nuclei ^{158}Er and ^{166}Yb therefore exhibit distinctive and complete S-shaped curves.

Generally S-shaped curves can be predicted theoretically by the Coriolis decoupling model of Stephens and Simon[9], and by calculations based on the CAP effect such as the two-level models of Sorensen[7] and of Krumlinde and Szymanski[6]. It should be emphasised that at the present stage however these models do not reproduce the experimental S-shaped curves quantitatively, but only give systematic trends as function of the deformation, the position of the Fermi level and the level density near the Fermi level. However the available data are not yet extensive enough to verify these trends and to give a clue as to which of the two physical pictures, namely the decoupling effect or the CAP effect, is responsible for the sudden increase in the moment of inertia.

Certain remarks are worthy of mention regarding the feeding mechanism in the $(\alpha, xn\gamma)$ reaction at $E_\alpha=100$ MeV. From the γ-intensities plotted as a function of spin in Figs. 4 and 9, it can be inferred that there exists hardly any side-feeding to levels up to the 6^+ state. The states between 8^+ and 20^+ receive all the side-feeding with a maximum feeding into the 10^+ and 12^+ state. Similarily Ward *et al.*[25] found in a study of the reactions ^{120,122,124}Sn(^{40}Ar, $4n$)^{156,158,160}Er, where states in the final nuclei up to 12^+ were observed, that side-feeding existed not into the first few excited states but only into the topmost two or three levels. Since from the present work on the $(\alpha, 8n)$ reaction the observed gsb levels extend now up to 18^+, the side-feeding is distributed over approximately six levels.

Consideration of the present experimental results shows that the decreasing anisotropy of the angular distributions can be interpreted as due to side-feeding. All stretched $E2$ transitions within a gsb must have the same angular distribution if there is no disturbing influence such as side-feeding or hyperfine interactions (HFI) with the nuclear environment[24]. It was observed experimentally that the anisotropy in

30 Mariscotti, M. A. J., Scharff-Goldhaber, G., Buck, B.: Phys. Rev. **178**, 1864 (1969).

^{158}Er (see Table 2) decreases as the γ-cascade develops down the gsb until the 6^+ state is reached and thereafter it remains constant. Because of this fact it is plausible to interpret the progressive change in the angular distributions as due to side-feeding[24], rather than due to HFI. If HFI were responsible, the anisotropy should continue to decrease for the lower transitions due to the increasing lifetimes encountered.

An additional perturbation of the angular distribution due to HFI may be expected for some ground state transitions deexciting the longer-lived 2^+ states. This can be seen by comparing the angular distribution data of ^{158}Er and ^{160}Er. No perturbation of the angular distribution of the $2^+ \rightarrow 0^+$ transition in ^{158}Er was observed where the first excited state has a halflife of 0.30 ns[22]. However the $2^+ \rightarrow 0^+$ transition in ^{160}Er has a somewhat reduced anisotropy (see Table 3) which can result from HFI since the halflife is 0.92 ns for the 2^+ state[22].

The authors thank Professor Amand Faessler for valuable discussions, Dr. U. Schwinn for the manufacture of the self-supporting metallic targets and Mr. Z. Seres for providing a computer code for analysis of two parameter spectra. In particular the technical help and assistance during the data collection provided by Mr. H. M. Jäger is gratefully appreciated. The authors would also like to acknowledge the support provided by the operating crew of the cyclotron.

Dr. R. M. Lieder
Dr. H. Beuscher
Dr. W. F. Davidson
Dr. P. Jahn
Mr. H.-J. Probst
Prof. Dr. C. Mayer-Böricke
Institut für Kernphysik
Kernforschungsanlage Jülich
D-5170 Jülich, Postfach 365
Federal Republic of Germany